Thermoreversible Ion Gels with Tunable Melting Temperatures from Triblock and Pentablock Copolymers

Yiyong He[†] and Timothy P. Lodge*[,†,‡]

Department of Chemistry and Department of Chemical Engineering and Materials Science, University of Minnesota, 207 Pleasant Street SE, Minneapolis, Minnesota 55455

Received September 20, 2007

ABSTRACT: We demonstrate a way to tune the critical gelation temperature (T_{gel}) for thermoreversible ion gels. Thermoreversible ion gels were prepared previously through the self-assembly of poly(*N*-isopropyl acrylamide-*b*-ethylene oxide-*b*-*N*-isopropyl acrylamide) (PNIPAm-PEO-PNIPAm) triblock copolymers in a room-temperature ionic liquid, 1-ethyl-3-methylimidazolium bis(trifluoromethylsulfonyl)imide ([EMIM][TFSI]). The resulting T_{gel} was 17 °C, as judged by the intersection of the dynamic moduli (G' and G'') at a fixed low frequency on increasing the temperature. These gels are of interest in various applications, including gate dielectric materials in organic field effect transistors. However, it is desirable to bring the T_{gel} significantly above room temperature in order to realize device applications. By incorporating solvatophobic blocks of polystyrene (PS) into the PNIPAm-PEO-PNIPAm triblock copolymers to produce well-defined PNIPAm-PS-PEO-PS-PNIPAm pentablock copolymers, we are able to adjust the T_{gel} of the resulting ion gels over a significant range (17−48 °C). We propose a melting mechanism for the PNIPAm-PS-PEO-PS-PNIPAm/[EMIM][TFSI] ion gels which involves two separate processes: (1) a thermodynamically controlled dissociation of the PNIPAm aggregates and (2) a dynamic exchange of PS blocks in and out of the PS micellar cores. The exchange dynamics of PS blocks in transient PS-PEO-PS/[EMIM][TFSI] ion gels were also studied, which are orders of magnitude slower than expected from intrinsic dynamics of bulk PS. This dynamic difference can be explained in the framework of hindered diffusion.

Introduction

Ion gels, a promising class of solid-state electrolytes, are made from swelling polymeric networks with ionic liquids and/or other functional components.[1−7] Due to the fascinating physicochemical properties possessed by room-temperature ionic liquids,[8−12] especially the high ionic conductivity and wide electrochemical window, ion gels have become attractive candidates as solid-state electrolytes with potential applications in electrochemical devices including lithium batteries,[13−16] organic thin-film transistors,[17] chemical sensors,[18] electromechanical actuators,[19−21] polymer light-emitting electrochemical cells,[22] and gas separation membranes.[23,24] Ion gels can overcome the leakage and flammability issues of organic solvent based electrolytes. Compared to traditional solid polymer electrolytes obtained by doping homopolymers with ions,[25,26] ion gels require significantly less polymer and thus offer improved ionic conductivity σ (e.g., on the order of 10 mS/cm).[2,7] Recently, we have shown that the capacitance of ion gels used as the gate dielectric in organic thin-film transistors (OTFT) can exceed 40 μF/cm^2 at 10 Hz, a value that is far larger than is achievable with typical inorganic or organic dielectric layers.[17] In addition, the large variety of cations and anions for ionic liquids afford unprecedented flexibility in materials design.

There have been relatively few reports describing ion gels. Rogers and co-workers prepared an ion gel by the cross-linking reaction of disuccinimidylpropyl poly(ethylene glycol) (PEG) monomers with four-arm tetraamine PEG cross-linkers.[1] Watanabe and co-workers successfully produced pyridinium and imidazolium salt based ion gels by in situ polymerization of vinyl monomers in ionic liquids.[2] Ion gels based on low molar mass gelators have also been described.[3] Recently, we reported an alternative way of developing ion gels through the self-assembly of ABA triblock copolymers, where the A blocks are insoluble and the B block is compatible with the chosen ionic liquid.[6] Transparent ion gels were achieved with as little as 4 wt % triblock copolymer and with σ nearly the same as that of the pure ionic liquid. The use of triblock copolymers produces well-defined physical gels through noncovalent association of A blocks, thereby offering appealing flexibility in controlling the gel microstructure and physical properties through variation of the copolymer block lengths, architecture, or identities.

We further developed a *thermoreversible* ion gel through the gelation of a poly(*N*-isopropyl acrylamide-*b*-ethylene oxide-*b*-*N*-isopropyl acrylamide) (PNIPAm-PEO-PNIPAm) triblock copolymer in the room-temperature ionic liquid 1-ethyl-3-methylimidazolium bis(trifluoromethylsulfonyl)imide ([EMIM][TFSI]).[7] In such physical gels, the cross-linking is reversible upon changing the temperature due to the temperature-dependent solubility of PNIPAm-end blocks in [EMIM][TFSI]. An upper critical solution temperature (UCST) response was observed in PNIPAm/[EMIM][TFSI] mixtures, whereby PNIPAm will phase separate from [EMIM][TFSI] at low temperatures.[4] However, the melting temperature (or critical gelation temperature T_{gel}) of the PNIPAm-PEO-PNIPAm/[EMIM][TFSI] ion gel lies just below room temperature, which limits its application. For example, in the case of OTFT, it would be desirable to have the T_{gel} well above room temperature, thereby allowing liquid-state processing for $T > T_{gel}$ but device performance under ambient conditions.

In this work, we demonstrate an adjustable melting temperature for a PNIPAm-PEO-PNIPAm/[EMIM][TFSI]-based ion gel by incorporating solvatophobic blocks, polystyrene (PS), into the triblock copolymer to create a PNIPAm-PS-PEO-PS−PNIPAm pentablock copolymer. A significant tuning range for T_{gel} is achieved by simply varying the molecular weight of the

* To whom correspondence should be addressed. E-mail: lodge@chem.umn.edu. Phone: (612) 625-0877. Fax: (612) 624-1589.
† Department of Chemistry.
‡ Department of Chemical Engineering and Materials Science.

10.1021/ma702014z CCC: $40.75
Published on Web 12/08/2007

Scheme 1. Synthesis of PS-PEO-PS Triblock and PNIPAm-PS-PEO-PS-PNIPAm Pentablock Copolymers

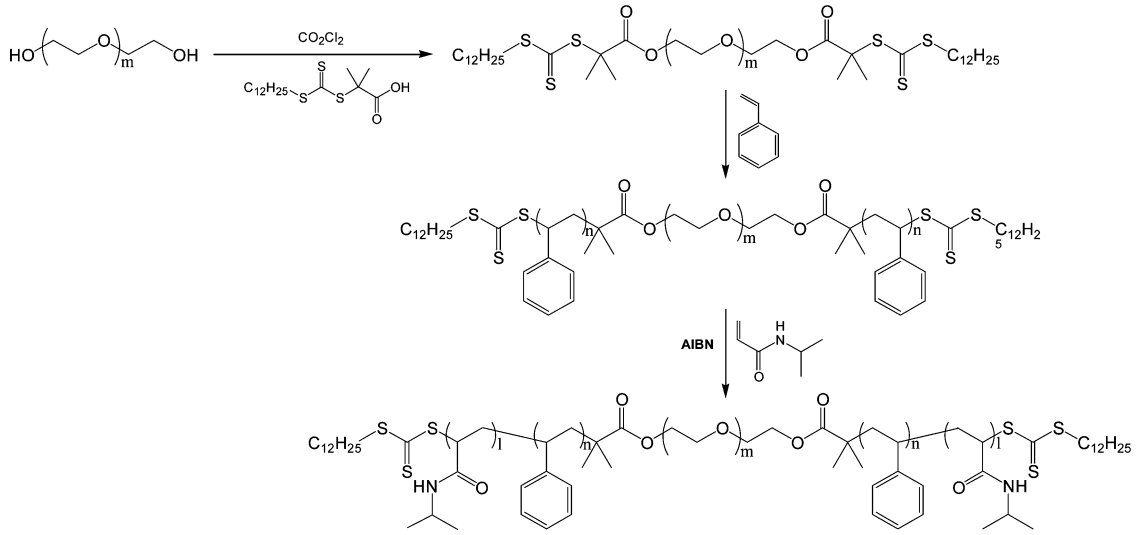

PS blocks (M_{PS}). A molecular mechanism is proposed for the gel melting process (sol−gel transition) in these pentablock copolymer ion gels. PS-PEO-PS/[EMIM][TFSI] ion gels with different M_{PS} were also studied to gain a deeper understanding of the dynamics of PS-end block exchange for transient gels. The paper is organized as follows. First, we describe the synthesis and characterization of the PS-PEO-PS triblock and PNIPAm-PS-PEO-PS-PNIPAm pentablock copolymers. Then we report the frequency dependence, temperature dependence, concentration dependence, hysteresis, and strain dependence of the linear viscoelastic moduli (storage modulus G' and loss modulus G'') of the triblock and pentablock copolymer based ion gels. The results are interpreted in terms of the mechanism and dynamics of the thermoreversible gelation.

Table 1. Molecular Characterization of NSOSN Pentablock Copolymers, SOS and NON Triblock Copolymers, and PEO Homopolymers

polymers	sample code	$M_{n,PS}$ (kDa)[a]	$M_{n,PNIPAm}$ (kDa)[b]	$M_{n,PEO}$ (kDa)	PDI
PNIPAm-PS-PEO-PS-PNIPAm	NSOSN-1	3.3	4.5	20	1.19
	NSOSN-2	3.8	4.4	35	1.25
PS-PEO-PS	SOS-1	3.3		20	1.11
	SOS-2	3.8		35	1.22
PNIPAm-PEO-PNIPAm[c]	NON		4.3	20	1.16
PEO	PEG-1			20	1.12
	PEG-2			35	1.12

[a] Determined by NMR. [b] Because of the overlapped resonance peaks of the PS and PNIPAm blocks, it is difficult to determine $M_{n,PNIPAm}$ by NMR. $M_{n,PNIPAm}$ was measured by GPC using PEO standards. [c] Reported in ref 7.

Experimental Section

Block Copolymers Synthesis and Characterization. Both the PS-PEO-PS triblock and PNIPAm-PS-PEO-PS-PNIPAm pentablock copolymers were synthesized by reversible addition−fragmentation chain transfer (RAFT) polymerization from a telechelic PEO precursor (Scheme 1). All reagents were used as received unless otherwise noted. 2,2′-Azobisisobutyronitrile (AIBN) and *N*-isopropylacrylamide (NIPAm) were purchased from Aldrich and purified by recrystallization from methanol and benzene/*n*-hexane (65/35 v/v), respectively. Styrene was passed through an activated alumina column prior to use. One PEG was purchased from Polymer Source, Inc. (M_n = 20 kDa), and the other was purchased from Aldrich (M_n = 35 kDa). Both polymers were purified by precipitation in *n*-hexane followed by drying in a vacuum oven. The chain transfer agent (CTA), (*S*)-1-dodecyl-(*S*′)-(α,α′-dimethyl-α″-acetic acid)-trithiocarbonate, was synthesized following a reported procedure.[27]

Here is a typical synthesis procedure for the pentablock copolymers. The telechelic PEO macroinitiator (CTA-PEO-CTA) was prepared as follows. CTA (1.0 g, 2.7×10^{-3} mol) was mixed with excess oxalyl chloride (1.5 g, 0.012 mol) in dry CH_2Cl_2 (4 mL) under argon atmosphere and stirred at room temperature until gas evolution stopped (∼2 h). Excess reagents were then removed under vacuum, and the residue was redissolved in dry CH_2Cl_2 (50 mL) followed by the addition of PEG (5.5 g, 2.7×10^{-4} mol). The reaction was allowed to proceed for 24 h at room temperature, after which the contents were precipitated four times in *n*-hexane (500 mL) and dried in a vacuum oven. The yield was 87%, with complete end group conversion.[28] Then, the CTA-PEO-CTA macroinitiator (1.1 g) and styrene (3 mL) were mixed in a high-pressure glass reactor, bubbled with argon for 15 min, sealed, and placed in an oil bath at 140 °C. After 40 min, the reaction was stopped by quenching the contents to ambient temperature. Most of the unreacted styrene was removed under vacuum, and the PS-PEO-PS product was further kept at 100 °C for 8 h to completely exhaust any residual styrene. The conversion of the styrene was 13%. To proceed to the PNIPAm-PS-PEO-PS-PNIPAm pentablock copolymer, PS-PEO-PS (1.2 g, 4.5×10^{-5} mol), NIPAm (2.2 g), AIBN (1.5 mg, 9.0×10^{-6} mol), and DMF (5 mL) were placed in a reactor, bubbled for 15 min, and reacted at 85 °C for 4 h. Most of the DMF was removed under vacuum. The residual mixture was diluted with CH_2Cl_2 (20 mL) and precipitated three times in *n*-hexane (200 mL). The yield was 2.0 g, with 40% conversion of NIPAm. Products with different PS and PNIPAm block lengths were achieved by controlling the reaction time and the amount of added monomer.

The product of each reaction step was confirmed by ^{1}H NMR spectroscopy and characterized by size exclusion chromatography (GPC) (Figures S1−S3 in the Supporting Information). Samples investigated in this work are listed in Table 1 along with the molecular weights of each block and the overall polydispersity (PDI). For simplicity, we denote the PNIPAm-PS-PEO-PS-PNIPAm pentablock and PS-PEO-PS and PNIPAm-PEO-PNIPAm triblock copolymers NSOSN, SOS, and NON, respectively, where S represents styrene, N represents *N*-isopropylacrylamide, and O represents oxyethylene.

Ionic Liquid and Ion Gel Preparation. The [EMIM][TFSI] ionic liquid was prepared following the synthesis protocol reported previously.[2] All ion gels were prepared by mixing weighed amounts of NSOSN pentablock (or SOS triblock) copolymer and ionic liquid and adding CH_2Cl_2 as a cosolvent. The concentration of copolymer was fixed at 10 wt % except for one NSOSN-1/[EMIM][TFSI] sample, which had 5 wt % copolymer. After the mixture has been stirred for 1 h, the cosolvent was removed by evaporation at ambient

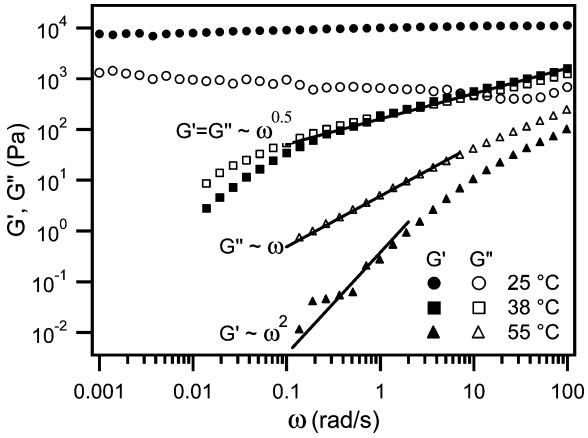

Figure 1. Frequency dependences of the dynamic shear moduli (G' and G'') for the ion gel with 10 wt % NSOSN-1 measured at a strain $\gamma = 2\%$ and three indicated temperatures. The solid lines are power law fits.

temperature for 24 h followed by placing the product in a vacuum oven at 70 °C until constant weight was achieved. To avoid any effects of moisture, all ion gel samples were subjected to vacuum pumping until no further weight loss was detected before measurements.

Rheology. Oscillatory shear measurements were performed on RFS II (Rheometric Fluids Spectrometer) and ARES (Rheometric Scientific) rheometers using the parallel plate geometry. Both 50 and 25 mm diameter plates were employed, depending on the modulus. A gap spacing of approximately 1 mm was used for all measurements. The gap was adjusted at each temperature to compensate for the thermal expansion of the tool set. The dynamic shear moduli (G' and G'') were examined in the linear viscoelastic regime (predetermined at each temperature). Temperatures were controlled to within ±0.2 °C of the set points.

Dynamic Light Scattering. The self-assembly of NSOSN and SOS in [EMIM][TFSI] was also investigated by dynamic light scattering (DLS) experiments on 1 wt % block copolymer/ionic liquid solutions. The solutions were passed through 0.20 μm filters into glass tubes with a diameter of 0.25 in. The DLS instrument is composed of a home-built goniometer, a Brookhaven BI-DS photomultiplier, a Lexel 95-2 Ar^+ laser operating at 488 nm, and a Brookhaven BI-9000 correlator. Temperatures were controlled to within ±0.2 °C using an index-matching silicon oil bath. Experiments were performed at various temperatures from 25 to 100 °C, and the intensity correlation functions $g_2(q,t)$ were recorded at five scattering angles between 60° and 120°. The hydrodynamic radius R_h was extracted using the Stokes−Einstein equation following the procedure described elsewhere.[29]

Results

Thermoreversible Gelation of NSOSN Pentablock Copolymers in [EMIM][TFSI]. Oscillatory shear measurements were performed on the NSOSN-1 ion gel with 10 wt % copolymer, over the temperature range of 25−55 °C. A strain amplitude of $\gamma = 2\%$ was used to ensure that the oscillatory shear measurements were taken in the linear viscoelastic regime. Representative data at 25, 38, and 55 °C are presented in Figure 1. At 55 °C, the sample is already a liquid. The storage modulus G' is significantly smaller than the loss modulus G'', and both exhibit power law dependencies on the angular frequency (ω) in the low-frequency window ($\omega\tau \ll 1$, where τ is the longest relaxation time of the polymer): $G' \sim \omega^2$ and $G'' \sim \omega$. This is the typical terminal rheological behavior of a viscoelastic fluid.[30] At 25 °C, the sample is a transparent free-standing gel. G' is larger than G'' and is nearly frequency independent, a characteristic of solidlike behavior. However, the steady increase in G'' with decreasing ω suggests a relaxation process at much lower frequencies. At 38 °C, the sample shows intermediate behavior; over the frequency range 0.1−100 rad/s there are similar magnitudes and power law dependences for G' and G'', $G' \approx G'' \sim \omega^{0.5}$. This is the signature of the transition between liquidlike and solidlike behavior and closely approximates the critical gelation point.[31,32] A separate, slow relaxation mode is observed at low frequencies (<0.1 rad/s), which has been commonly seen in physical gels with weak interactions near T_{gel}.[33] Intermediate power law dependences were observed for other temperatures between 25 and 55 °C; these data are not included in Figure 1 for the sake of clarity.

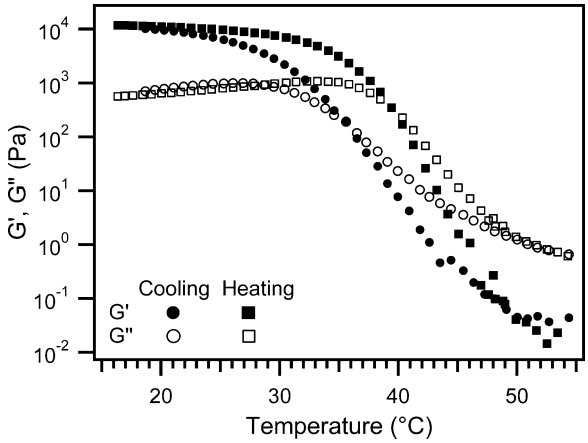

Figure 2. Dynamic shear moduli (G' and G'') as a function of temperature measured in a heating−to−cooling thermal cycle for the ion gel with 10 wt % NSOSN-1. The measurements were taken at a strain $\gamma = 2\%$ and frequency $\omega = 0.1$ rad/s with heating and cooling rates of ±1 °C/min.

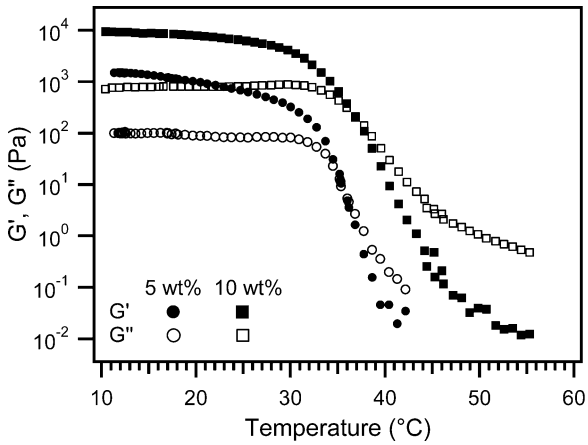

Figure 3. Temperature-dependent dynamic shear moduli (G' and G'') for the two NSOSN-1 ion gels with different copolymer concentrations measured at a strain $\gamma = 2\%$, frequency $\omega = 0.1$ rad/s, and heating rate = 1 °C/min.

A further manifestation of the thermoresponsive sol−gel transition is shown in Figure 2, in which the dynamic shear moduli were measured during isochronal temperature sweeps from 15 to 55 °C in a heating−to−cooling thermal cycle. It clearly shows that there are transitions for both G' and G'' as a function of temperature, with the net change in G' approaching 6 orders of magnitude. A hysteresis loop was also observed. For the heating process, T_{gel} (determined from the crossing of the G' and G'' curves) is around 39 °C, consistent with the results in Figure 1.

In Figure 3, the temperature-dependent dynamic shear moduli of two NSOSN-1 ion gels with 5 and 10 wt % copolymer are compared. In both cases, G' decreases significantly upon heating, indicating gel melting. T_{gel} of the 5 wt % ion gel is only 3 °C

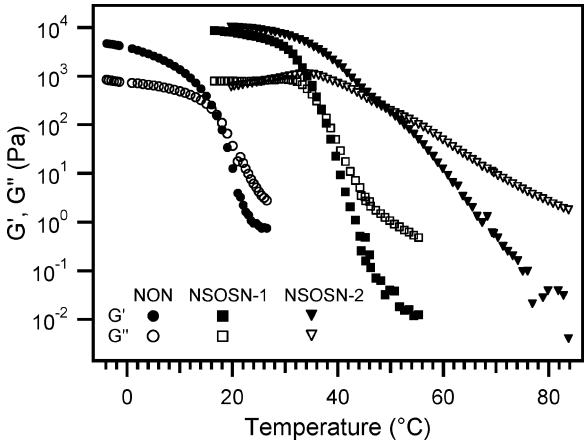

Figure 4. Temperature-dependent dynamic shear moduli (G' and G'') for three ion gels (NON, NSOSN-1, and NSOSN-2, each with 10 wt % copolymer in [EMIM][TFSI]). The measurements were taken at a strain $\gamma = 2\%$, frequency $\omega = 0.1$ rad/s, and heating rate = 1 °C/min.

below that of the 10 wt % ion gel. The weak concentration dependence of T_{gel} is consistent with the reported UCST phase diagram of PNIPAm/[EMIM][TFSI] mixtures[4] and is similar to the gelation behavior of aqueous solutions of PNIPAm-based copolymers (which, interestingly, show a lower critical solution temperature (LCST) behavior).[34] As expected, both G' and G'' of the 10 wt % ion gel are greater than those of the 5 wt % ion gel. The concentration dependence of the plateau modulus is in agreement with the typical scaling law for gels, $G' \sim \phi^{2.3}$, where ϕ is the concentration of polymer.[35]

We also investigated the rheological response of the NSOSN-1 ion gel under large strains (Figure S4 of Supporting Informaion). Dynamic strain sweep experiments were conducted over a wide range of γ up to the instrument limit. Within the γ range of our experiments (>40%), the ion gel displays linear viscoelastic response (G' remains invariant with respect to γ), indicating no break up of the gel microstructure.

Ion Gels with Tunable Melting Temperatures. In a recent work, we reported a thermoreversible ion gel by the self-assembly of a NON triblock copolymer in [EMIM][TFSI].[7] However, the T_{gel} of the ion gel was below room temperature (~17 °C), which limits its application. The current work extends this approach, with the goal of tuning the T_{gel} of PNIPAm copolymer based ion gels. The temperature-dependent shear moduli of three ion gels (NON, NSOSN-1, and NSOSN-2, each with 10 wt % copolymer in [EMIM][TFSI]) are summarized in Figure 4. To simplify interpretation, we have matched the molecular weights of the PNIPAm blocks in the three copolymers. The molecular weights of the PEO blocks in NON and NSOSN-1 are also the same. It is clear in Figure 4 that, by incorporating solvatophobic blocks (PS) into NON chains, the T_{gel} increases by 20 °C from the NON to the NSOSN-1 ion gels. We can increase the T_{gel} by another 10 °C using longer PS blocks (from the NSOSN-1 to the NSOSN-2 ion gels). Thus, a significant tuning range for the T_{gel} (17−48 °C) was achieved in PNIPAm copolymer based ion gels by adding solvatophobic blocks and varying their molecular weight. Note that 48 °C is significantly above the anticipated use temperature for "plastic electronics" yet is low enough that the processing of organic components above T_{gel} is quite feasible.

Having achieved the goal of tuning T_{gel} for PNIPAm copolymer based ion gels, we now consider the interesting "double melting" phenomenon in the NSOSN-2 ion gel, as indicated by two shoulders in the temperature dependence of G' (Figure 4). We speculate that the first transition has the same

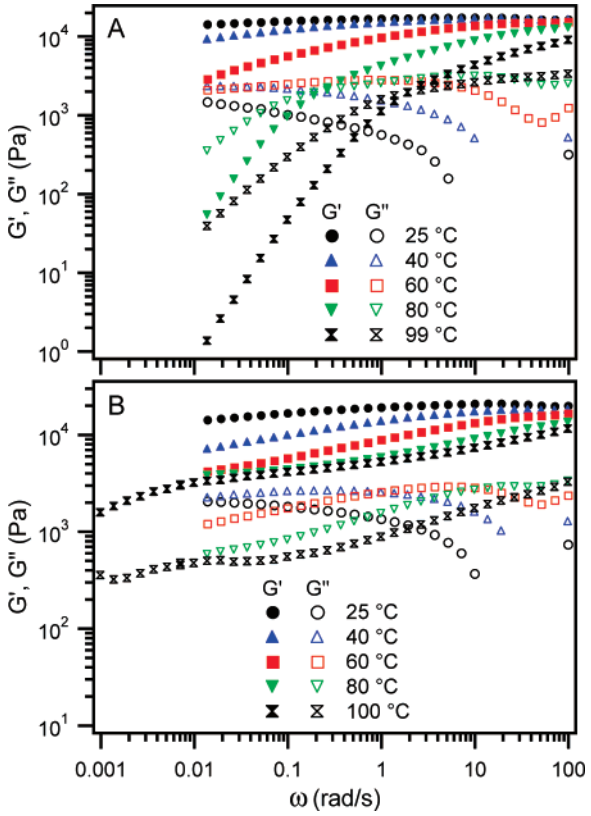

Figure 5. Frequency dependencies of the dynamic shear moduli (G' and G'') for the two ion gels measured at a strain $\gamma = 2\%$ and the indicated temperatures: (A) 10 wt % SOS-1; (B) 10 wt % SOS-2.

thermodynamic origin as the NON ion gel, i.e., dissolution of the PNIPAm blocks above the UCST phase boundary, and that the second transition is a dynamic process pertaining to transient networks, i.e., exchange of the PS blocks between PS micellar cores. To verify the existence of transient networks cross-linked by weakly aggregated PS blocks, we investigated the gelation of SOS triblock copolymers in [EMIM][TFSI] in more detail.

Gelation of SOS Triblock Copolymers in [EMIM][TFSI]. Figure 5 shows G' and G'' as a function of frequency for two SOS ion gels over a temperature range 25−100 °C. The SOS-2 triblock copolymer has a larger M_{PS} than the SOS-1. These results are reversible in the sense that the low-temperature behavior is recovered after cooling from the highest temperatures.

Rubberlike behavior is observed for the SOS-2 ion gel over the entire investigated temperature range, as indicated by $G' > G''$ and weak frequency-dependent plateaus in G' (Figure 5B).[36] Qualitatively, the results are similar to an SOS/[BMIM][PF_6] ion gel that we examined previously.[6] The plateaus at lower frequencies can be interpreted as reflecting a network structure, cross-linked by the PS micellar cores. At higher frequencies, there is evidence of a second relaxation process, which is attributed to the relaxation of the network strands, i.e., the PEO blocks. On closer inspection, the plateau modulus (G_e) decreases with increasing temperature. G_e of a polymer network is equal to kT per elastically effective network strand, $G_e = \nu kT$, where ν is the number density of network strands and k is the Boltzmann constant. One direct consequence of this entropic elasticity is that G_e increases with temperature if no change happens to the network structure. In contrast to permanent chemical cross-links, for which G_e increases with temperature, G_e of physical gels often decreases on heating. Such behavior

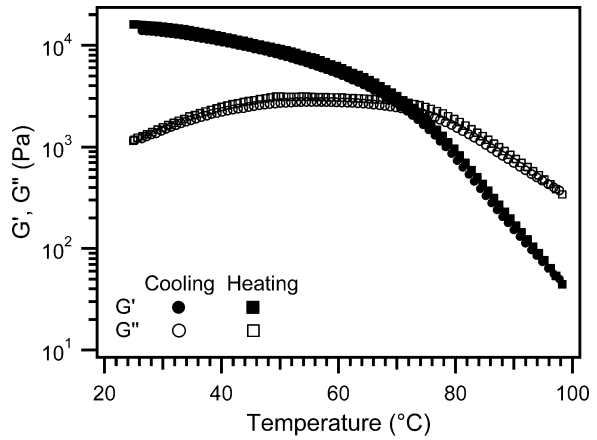

Figure 6. Dynamic shear moduli (G' and G'') as a function of temperature in a heating−to−cooling thermal cycle for the ion gel with 10 wt % SOS-1. The measurements were taken at a strain $\gamma = 2\%$ and frequency $\omega = 0.1$ rad/s with heating and cooling rates of ± 1 °C/min.

is due to faster relaxation of the physical cross-links which releases the network stress more effectively on heating.

The terminal flow behavior of the transient SOS network is better demonstrated in Figure 5A due to the shorter PS-end blocks in SOS-1. In the experimental time window, a viscoelastic liquidlike behavior is observed for the SOS-1 ion gel at temperatures above 60 °C, as evidenced by $G' < G''$ and power law exponents of two and one for G' and G'', respectively.[30] A further manifestation of the flow behavior is shown in Figure 6, in which G' and G'' were measured during isochronal temperature sweeps from 25 to 100 °C in a heating−to−cooling thermal cycle. It shows a T_{gel} of 70 °C at the measuring frequency. Another feature is that there is almost no hysteresis in Figure 6, indicating that the SOS ion gels have quite distinct "melting" mechanism than the PNIPAm copolymer based ion gels.

The terminal flow behavior of the SOS-1 ion gel upon heating can be explained by the transient network theory. Transient networks and their rheological features have been extensively studied for ABA triblock copolymers in a midblock selective solvent.[33,37−41] Under conditions where the associating strength of the A chains is weak (the solvent is not too poor for A) and A chains are allowed to reversibly associate or dissociate from the cross-linking points (above T_g of A aggregates), a transient ABA network is formed and its viscoelastic properties strongly depend on a finite dissociation time (terminal relaxation time τ_1). Technically, gels from transient networks must be classified as viscoelastic liquids although τ_1 may be extraordinarily large. In order to achieve this state, it is convenient to conduct the experiments near the critical micelle temperature or using ABA triblock copolymers with very short A-end blocks. In both cases, the association strength of the terminal blocks is not strong enough to generate a very long-lived network. Since SOS-2 has a larger M_{PS} than SOS-1, τ_1 of the SOS-2 ion gel is beyond the experimental timescale and the terminal flow regime cannot be accessed.

Discussion

Controlling Gel Melting Temperatures. There are at least two possible ways to increase the melting temperatures of NON ion gels: (1) by increasing the molecular weight of the PNIPAm-end blocks and (2) by copolymerizing NIPAm with a solvatophobic monomer. The first method appears straightforward in light of the molecular-weight-dependent UCST phase behavior of PNIPAm/[EMIM][TFSI] mixtures.[4] However, due to the weak molecular weight dependence of the phase boundary, only a limited tuning range can be achieved in this way, so we pursued the second route here.[5] There have been many reports of controlled phase separation temperatures of homopolymers in a given solvent by copolymerizing with a solvatophobic or solvatophilic monomer.[5,42,43] Here, we applied the same principle to triblock copolymers and have shown that we are able to tune the melting temperatures of thermoresponsive PNIPAm copolymer based ion gels. A T_{gel} tuning range as large as 30 degrees was achieved, demonstrating a promising way to control gel melting temperature, which could be extended to other triblock copolymer gels.

There is, however, an effective limit of the molecular weight of PS blocks (M_{PS}). The incorporation of larger M_{PS} will reduce the temperature sensitivity of the PNIPAm blocks. A direct consequence is a loss of sharpness in the phase transition. The critical M_{PS} to retain the thermoresponsiveness is around 4 kDa. We tested a NSOSN pentablock copolymer with $M_{PS} = 4.9$ kDa, and it behaves just like a SOS triblock copolymer and completely loses the thermoresponsiveness of the NON triblock copolymer (results not shown). One possibility to overcome this limitation would be to make a PS−PNIPAm random copolymer instead of a block copolymer. In this way, we might expect to obtain an even larger tuning range for the T_{gel}. For this particular system, there is a technical challenge, however, due to the significant difference in the reactivity ratios of styrene and NIPAm monomers, but it should be feasible by choosing an appropriate solvatophobic monomer.

Molecular Mechanism of the Thermoreversible Gelation. As implied by the two shoulders in $G'(T)$ associated with the melting process of the NSOSN-2 ion gel (Figure 4), NSOSN ion gels have a different thermoreversible gelation mechanism than the NON ion gels. A schematic illustration of the thermoreversible sol−gel transitions for both ion gels is shown in Figure 7. In the case of NON triblock copolymers, the gel melting is simply due to the largely entropically driven dissociation of the PNIPAm micellar cores, a mechanism that has been well established in many "thermoplastic elastomer" systems.[44] After gel melting, the system changes quite sharply from a micellar network to a block copolymer solution. For the NSOSN pentablock copolymers, we assume that core−shell−corona micelles are formed in [EMIM][TFSI] below the T_{gel}, with the PNIPAm blocks forming the micellar cores and the PS blocks the shells.[45,46] Two separate processes are then involved in gel melting, which correspond to the two $G'(T)$ features observed in the NSOSN-2 ion gel (Figure 4): (1) thermodynamic dissociation of the PNIPAm aggregates and (2) dynamic exchange of the PS blocks in and out of the PS cores. The two processes may occur at roughly the same temperature (in the case of NSOSN-1 ion gel) or sequentially (in the case of NSOSN-2 ion gel), depending on their relative timescales. After melting the PNIPAm aggregates, the system changes from a locked micellar network to a transient micellar network. We should anticipate a similar melting behavior for SNONS ion gels.

To confirm this proposed dual melting mechanism for the pentablock copolymer ion gels, DLS measurements were conducted on a dilute NSOSN-1 solution with 1 wt % copolymer over the temperature range 25−100 °C. Following a previously described procedure,[29] the apparent hydrodynamic radius R_h of the self-assembled NSOSN-1 as well as its distribution (by the CONTIN Laplace inversion program) was extracted. We found almost no temperature dependence for the average micelle size $\langle R_h \rangle$, and the scattering intensity only decreases by about 20%

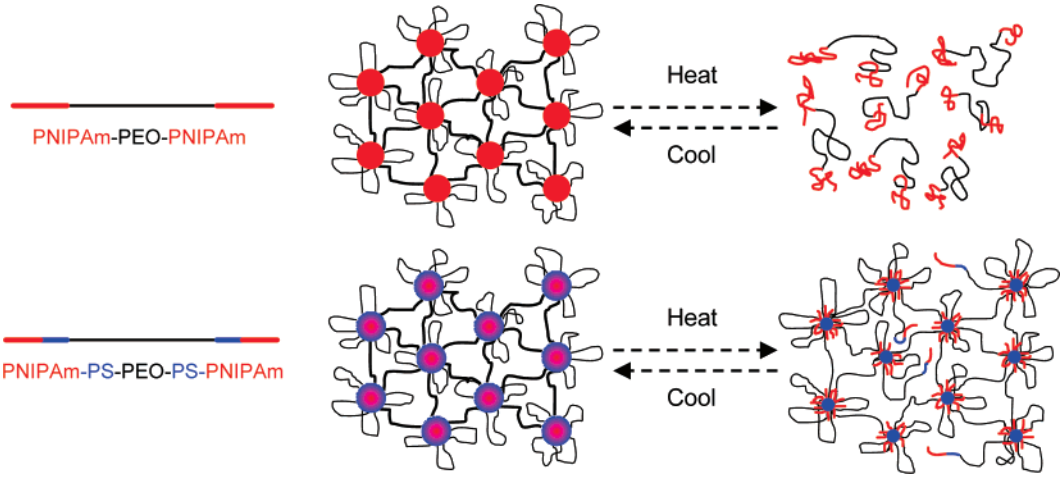

Figure 7. Schematic illustration of the thermoreversible sol−gel transitions in the NON and NSOSN ion gels. In the latter case, more dangling chains are formed on heating due to the exchange of PS blocks.

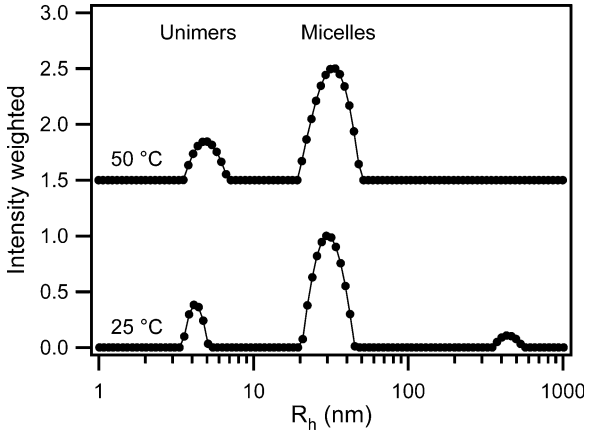

Figure 8. Hydrodynamic radius distribution for a 1 wt % NSOSN-1/[EMIM][TFSI] solution measured by DLS at a scattering angle of 90 °.

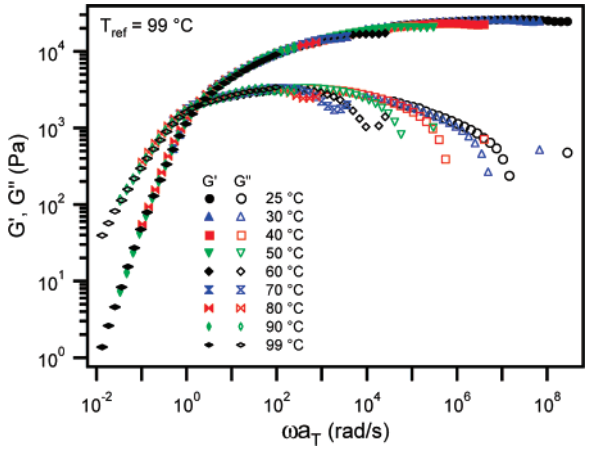

Figure 9. Time−temperature superposition of the dynamic shear moduli (G' and G'') for the transient ion gel with 10 wt % SOS-1 (data in Figure 5A).

upon heating to temperatures above the T_{gel}. Representative data for R_h at two temperatures are presented in Figure 8. The peak around 30 nm is ascribed to the flowerlike NSOSN-1 micelles, and the peak around 5 nm is assigned to free NSOSN-1 chains. Because of the weak scattering intensity, we do not attribute any significance to the small peak around 450 nm. The micellar peak almost remains unchanged irrespective of temperature up to at least 100 °C, supporting the gel melting picture in Figure 7. The observed free block copolymer chains are consistent with the conclusion in the previous section that the PS block aggregates are not strongly bound. Thus the exchange of PS blocks in and out of PS aggregates is possible, and the dynamics of this exchange process are further analyzed and discussed below.

Other evidence supporting the two-step gel melting process was found in a hysteresis study. The same thermal cycling experiments as presented in Figures 2 and 6 were also performed on the NSOSN-2 ion gel. There is a hysteresis loop for the first $G'(T)$ transition, but no hysteresis was observed for the second $G'(T)$ transition, indicating quite different molecular mechanisms for the two separate processes. (Figure S6 in the Supporting Information)

Exchange Dynamics of PS Blocks in Transient Gels. The exchange of PS blocks in and out of the PS aggregates is observable in the transient SOS-1 ion gels. Such exchange allows the SOS-1 triblock copolymer network to flow under deformation with the terminal relaxation time dependent on temperature, as observed in the rheology measurements (Figures 5A and 6). In the following, we focus on the transient SOS-1 ion gel to investigate the exchange dynamics of PS blocks.

Tanaka and Edwards developed a transient network theory which considers telechelic polymers having associative groups at their chain ends.[37] When a chain is dissociated from a junction, either by thermal motion or by tension, it must overcome an energy barrier for the chain to dissociate and diffuse into the surrounding matrix. Their theory is suitable to describe transient networks made up of ABA triblock copolymers with associative A chains. In our case, the energy barrier depends on the incompatibility $(\chi - {}^1/_2)N$ between the solvent and the end block, where χ is the Flory−Huggins interaction parameter and N is the degree of polymerization of the end block. The temperature dependence of the segmental mobility will also play a role. Therefore, the terminal relaxation time of the transient gel ($\tau_{1,gel}$) should increase with increasing end block length and with decreasing temperature (for solutions with UCST phase behavior).

First, we analyzed the temperature dependence of the terminal relaxation of the SOS-1 transient gel, obtained by time−temperature superposition of the slower relaxation mode in G' and G''. The time−temperature superposition of G' and G'' of the 10 wt % SOS-1 transient gel (data in Figure 5A) is presented in Figure 9. A reasonably good master curve was achieved for the slower motions. Terminal relaxation behavior with G' and G'' increasing with the second and first powers of ω, respec-

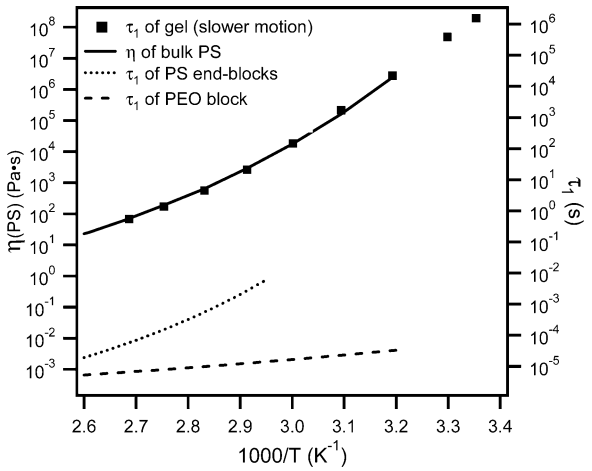

Figure 10. Temperature-dependent terminal relaxation times (τ_1) of the transient SOS-1 ion gel with 10 wt % copolymer. The viscosity data of a bulk PS sample (η) are presented to compare the temperature dependencies. The longest relaxation times of PS and PEO blocks in SOS-1 chains are also estimated and compared to the terminal relaxation times of the SOS-1 transient network in the ionic liquid.

tively, was clearly observed in the master curve. The viscoelastic spectrum is actually reminiscent of entangled star polymers,[47] where the further increase of G'' beyond the crossover frequency reflects the exponentially retarded longer relaxation modes of the arms. At the reference temperature $T_{ref} = 99$ °C, the transient gel has a $\tau_{1,gel}$ of 0.55 s, as conventionally determined by the crossover frequency (ω_c) at which the G' and G'' values are equal, $\tau_{1,gel} = \omega_c^{-1}$. $\tau_{1,gel}$ of the transient gel at various temperatures were calculated from the shift factors (a_T) and plotted in Figure 10 (vs right axis). The temperature-dependent viscosity of a bulk PS sample (η_{PS}) is also shown in the same plot (vs left axis). The temperature dependence of $\tau_{1,gel}$ closely tracks that of η_{PS}, verifying that the terminal relaxation of the transient gel is related to the motion of the PS-end blocks. In constructing Figure 10, η_{PS} was taken from ref 48 but shifted to lower temperatures by 70 K. Thus the data presented in Figure 10 are roughly equivalent to that of a bulk PS sample with $T_g \approx 25$ °C. This suppression of T_g is not unexpected taking into account the low M_{PS}, the nanoscopic PS domains,[49] and the plasticizing effect on the PS cores in the surrounding matrix (PEO plus ionic liquid).

The terminal relaxation of the transient gel depends both on the thermodynamic penalty for pulling the PS blocks through the ionic liquid and on the intrinsic mobility of PS. In Figure 10, the terminal relaxation times of the PS-end block ($\tau_{1,PS}$) and of the PEO midblock ($\tau_{1,PEO}$) in SOS triblock copolymer chains were plotted together with $\tau_{1,gel}$. $\tau_{1,PEO}$ values were taken from the results of bulk PEO reported in ref 50 and adjusted based on the experimentally established scaling law:[51] $\tau_1 \sim N^{3.4}$. Since the T_g of PEO (−78 °C) is close to that of [EMIM][TFSI] (−86 °C), we anticipate that $\tau_{1,PEO}$ will not be significantly affected by the ionic liquid solvation. $\tau_{1,PS}$ was calculated from the segmental dynamics (τ_{seg}) of bulk PS[52] (with T_g equivalent to that of the micellar cores, 25 °C) based on the empirical relationship:[53,54] $(\tau_1/\tau_{seg}) \approx N^2$. Both the magnitude and the temperature dependence of $\tau_{1,gel}$ are significantly different than those of $\tau_{1,PEO}$, which excludes a direct correlation between them. As expected from the previous discussion, $\tau_{1,gel}$ and $\tau_{1,PS}$ have similar temperature dependencies. However, $\tau_{1,gel}$ is 4 orders of magnitude larger than $\tau_{1,PS}$, the intrinsic terminal relaxation time of PS blocks.

This dynamic difference may be ascribed to the thermodynamic penalty for the exchange of PS blocks and can be quantified in the framework of "hindered diffusion".[55−57] Under the hindered diffusion mechanism, the diffusion coefficient D is given by

$$D \approx D_0 \exp\left[-A\left(\chi - \frac{1}{2}\right)N_A\right] \quad (1)$$

where D_0 is the diffusion coefficient in the absence of any interactions, A is a prefactor of order unity, and N_A is the number of monomers referenced to the solvent molecular volume (the average size of the cation and the anion of the ionic liquid in our case). From eq 1, the characteristic relaxation time for the PS block exchange can be expressed as

$$\tau_{1,gel} \approx \tau_{1,PS} \exp\left[A\left(\chi - \frac{1}{2}\right)N_{PS}\right] \quad (2)$$

By assuming $A = 1$, we obtain $\chi \approx 0.88$ from eq 2, which is a reasonable value.

Conclusions

We have demonstrated tuning of the critical gelation temperatures (T_{gel}) of triblock copolymer based thermoreversible ion gels. By incorporating solvatophobic blocks (PS) into the PNIPAm-PEO-PNIPAm triblock copolymers to produce the well-defined PNIPAm-PS-PEO-PS-PNIPAm pentablock copolymers, we were able to adjust the T_{gel} of the resulting ion gels. A significant tuning range for the T_{gel} (17−48 °C) was achieved by varying the molecular weight of the PS blocks. The methodology for controlling the T_{gel} of thermoreversible ion gels elaborated in this work should provide an impetus for the utilization of these materials in a broader spectrum of applications. The same principle could be extended to other thermoreversible polymer gels as well.

The PNIPAm-PS-PEO-PS-PNIPAm/[EMIM][TFSI] ion gels have a more complicated melting mechanism than the PNIPAm-PEO-PNIPAm/[EMIM][TFSI] ion gels described previously. For the pentablock copolymer based ion gels, two separate processes are involved in the gel melting: (1) dissociation of the PNIPAm aggregates (a thermodynamic transition) and (2) dynamic exchange of PS blocks in and out of the PS micellar cores (a kinetic process). The two processes may occur concurrently or sequentially, depending on their characteristic timescales at the temperature of interest. The exchange dynamics of PS blocks were further studied in transient PS-PEO-PS/[EMIM][TFSI] ion gels. Because of the thermodynamic penalty for pulling the PS blocks through the ionic liquid, the exchange dynamics of PS blocks are orders of magnitude slower than what would be expected from the intrinsic dynamics of bulk PS. The dynamic difference can be explained in the framework of hindered diffusion.

Acknowledgment. This work was supported by the National Science Foundation through Award DMR-0406656.

Supporting Information Available: The GPC traces and NMR spectra of all synthesized products and their precursors, strain dependence of the dynamic shear moduli for the NSOSN-1 ion gel, comparison of the gel melting processes for four ion gels (NON, NSOSN-1, NSOSN-2, and SOS-1), hysteresis in the melting process of the NSOSN-2 ion gel, and shift factors from the time−temperature superposition of the slow mode relaxation in the SOS-2

ion gel. This material is available free of charge via the Internet at http://pubs.acs.org.

References and Notes

(1) Klingshirn, M. A.; Spear, S. K.; Subramanian, R.; Holbrey, J. D.; Huddleston, J. G.; Rogers, R. D. *Chem. Mater.* **2004**, *16*, 3091−3097.
(2) Susan, M. A. B. H.; Kaneko, T.; Noda, A.; Watanabe, M. *J. Am. Chem. Soc.* **2005**, *127*, 4976−4983.
(3) Hanabusa, K.; Fukui, H.; Suzuki, M.; Shirai, H. *Langmuir* **2005**, *21*, 10383−10390.
(4) Ueki, T.; Watanabe, M. *Chem. Lett.* **2006**, *35*, 964−965.
(5) Ueki, T.; Watanabe, M. *Langmuir* **2007**, *23*, 988−990.
(6) He, Y.; Boswell, P. G.; Bühlmann, P.; Lodge, T. P. *J. Phys. Chem. B* **2007**, *111*, 4645−4652.
(7) He, Y.; Lodge, T. P. *Chem. Commun.* **2007**, 2732−2734.
(8) Huddleston, J. G.; Visser, A. E.; Reichert, W. M.; Willauer, H. D.; Broker, G. A.; Rogers, R. D. *Green Chem.* **2001**, *3*, 156−164.
(9) Welton, T. *Chem. Rev.* **1999**, *99*, 2071−2083.
(10) Hoffmann, M. M.; Heitz, M. P.; Carr, J. B.; Tubbs, J. D. *J. Dispersion Sci. Technol.* **2003**, *24*, 155−171.
(11) Lee, S. G. *Chem. Commun.* **2006**, 1049−1063.
(12) Anderson, J. L.; Ding, J.; Welton, T.; Armstrong, D. W. *J. Am. Chem. Soc.* **2002**, *124*, 14247−14254.
(13) Shobukawa, H.; Tokuda, H.; Tabata, S.; Watanabe, M. *Electrochim. Acta* **2004**, *50*, 305−309.
(14) Shin, J. H.; Henderson, W. A.; Passerini, S. *J. Electrochem. Soc.* **2005**, *152*, A978−A983.
(15) Shin, J. H.; Henderson, W. A.; Passerini, S. *Electrochem. Commun.* **2003**, *5*, 1016−1020.
(16) Christie, A. M.; Lilley, S. J.; Staunton, E.; Andreev, Y. G.; Bruce, P. G. *Nature* **2005**, *433*, 50−53.
(17) Lee, J.; Panzer, M. J.; He, Y.; Lodge, T. P.; Frisbie, C. D. *J. Am. Chem. Soc.* **2007**, *129*, 4532−4533.
(18) Boswell, P. G.; Lugert, E. C.; Rabai, J.; Amin, E. A.; Bühlmann, P. *J. Am. Chem. Soc.* **2005**, *127*, 16976−16984.
(19) Fukushima, T.; Kosaka, A.; Yamamoto, Y.; Aimiya, T.; Notazawa, S.; Takigawa, T.; Inabe, T.; Aida, T. *Small* **2006**, *2*, 554−560.
(20) Zhou, D.; Spinks, G. M.; Wallace, G. G.; Tiyapiboonchaiya, C.; MacFarlane, D. R.; Forsyth, M.; Sun, J. Z. *Electrochim. Acta* **2003**, *48*, 2355−2359.
(21) Akle, B. J.; Bennett, M. D.; Leo, D. J. *Sens. Actuators, A* **2006**, *126*, 173−181.
(22) Shao, Y.; Bazan, G. C.; Heeger, A. J. *Adv. Mater.* **2007**, *19*, 365−370.
(23) Huang, J.; Riisager, A.; Wasserscheid, P.; Fehrmann, R. *Chem. Commun.* **2006**, 4027−4029.
(24) Tang, J. B.; Tang, H. D.; Sun, W. L.; Plancher, H.; Radosz, M.; Shen, Y. Q. *Chem. Commun.* **2005**, 3325−3327.
(25) Singh, B.; Sekhon, S. S. *J. Phys. Chem. B* **2005**, *109*, 16539−16543.
(26) Lewandowski, A.; Swiderska, A. *Solid State Ionics* **2004**, *169*, 21−24.
(27) Lai, J. T.; Filla, D.; Shea, R. *Macromolecules* **2002**, *35*, 6754−6756.
(28) The conversion was determined from the relative intensity of the PEO and CTA resonance peaks in NMR spectrum with the molecular weight of the starting PEG as a reference.
(29) He, Y.; Li, Z.; Simone, P. M.; Lodge, T. P. *J. Am. Chem. Soc.* **2006**, *128*, 2745−2750.
(30) Larson, R. G. *The Structure and Rheology of Complex Fluids*; Oxford University Press: New York, 1999.
(31) Winter, H. H.; Chambon, F. *J. Rheol.* **1986**, *30*, 367−382.
(32) Chambon, F.; Petrovic, Z. S.; MacKnight, W. J.; Winter, H. H. *Macromolecules* **1986**, *19*, 2146−2149.
(33) Sato, T.; Watanabe, H.; Osaki, K. *Macromolecules* **2000**, *33*, 1686−1691.
(34) Wu, C.; Wang, X. H. *Phys. Rev. Lett.* **1998**, *80*, 4092−4094.
(35) Kobayashi, K.; Huang, C. I.; Lodge, T. P. *Macromolecules* **1999**, *32*, 7070−7077.
(36) Rubinstein, M.; Colby, R. H. *Polymer Physics*; Oxford University Press: New York, 2003.
(37) Tanaka, F.; Edwards, S. F. *Macromolecules* **1992**, *25*, 1516−1523.
(38) Seitz, M. E.; Burghardt, W. R.; Faber, K. T.; Shull, K. R. *Macromolecules* **2007**, *40*, 1218−1226.
(39) Inomata, K.; Nakanishi, D.; Banno, A.; Nakanishi, E.; Abe, Y.; Kurihara, R.; Fujimoto, K.; Nose, T. *Polymer* **2003**, *44*, 5303−5310.
(40) Vega, D. A.; Sebastian, J. M.; Loo, Y. L.; Register, R. A. *J. Polym. Sci., Part B: Polym. Phys.* **2001**, *39*, 2183−2197.
(41) Mai, S. M.; Ludhera, S.; Heatley, F.; Attwood, D.; Booth, C. *J. Chem. Soc., Faraday Trans.* **1998**, *94*, 567−572.
(42) Takei, Y. G.; Aoki, T.; Sanui, K.; Ogata, N.; Okano, T.; Sakurai, Y. *Bioconjugate Chem.* **1993**, *4*, 341−346.
(43) Ueki, T.; Karino, T.; Kobayashi, Y.; Shibayama, M.; Watanabe, M. *J. Phys. Chem. B.* **2007**, *111*, 4750−4754.
(44) Drzal, P. L.; Shull, K. R. *Macromolecules* **2003**, *36*, 2000−2008.
(45) Chou, S. H.; Tsao, H. K.; Sheng, Y. J. *J. Chem. Phys.* **2006**, *125*.
(46) According to ref 45, other micellar morphologies (including incomplete skin-layered micelles or bicore micelle) are also possible. We can draw a similar picture to Figure 7 and all following arguments still work as well.
(47) Milner, S. T.; McLeish, T. C. B. *Macromolecules* **1997**, *30*, 2159−2166.
(48) Chapman, B. R.; Hamersky, M. W.; Milhaupt, J. M.; Kostelecky, C.; Lodge, T. P.; von Meerwall, E. D.; Smith, S. D. *Macromolecules* **1998**, *31*, 4562−4573.
(49) Roth, C. B.; Dutcher, J. R. *J. Electroanal. Chem.* **2005**, *584*, 13−22.
(50) Colby, R. H. *Polymer* **1989**, *30*, 1275−1278.
(51) Ferry, J. *Viscoelastic properties of polymers*, 3rd ed.; Wiley: New York, 1980.
(52) He, Y.; Lutz, T. R.; Ediger, M. D.; Ayyagari, C.; Bedrov, D.; Smith, G. D. *Macromolecules* **2004**, *37*, 5032−5039.
(53) Roland, C. M.; Ngai, K. L.; Santangelo, P. G.; Qiu, X. H.; Ediger, M. D.; Plazek, D. J. *Macromolecules* **2001**, *34*, 6159−6160.
(54) He, Y.; Lutz, T. R.; Ediger, M. D.; Lodge, T. P. *Macromolecules* **2003**, *36*, 9170−9175.
(55) Cavicchi, K. A.; Lodge, T. P. *Macromolecules* **2003**, *36*, 7158−7164.
(56) Yokoyama, H.; Kramer, E. J. *Macromolecules* **1998**, *31*, 7871−7876.
(57) Hotta, A.; Clarke, S. M.; Terentjev, E. M. *Macromolecules* **2002**, *35*, 271−277.

MA702014Z